Supramolecular Silanol Chemistry in the Gas Phase. Topological (AIM) and Population (NBO) Analyses of Hydrogen-Bonded Complexes between H₃SiOH and Selected O- and N-Acceptor Molecules

Jens Beckmann* and Simon Grabowsky

Institut für Chemie und Biochemie, Freie Universität Berlin, Fabeckstrasse 34−36, 14195 Berlin, Germany

Received: November 4, 2006; In Final Form: December 23, 2006

Hydrogen bonding of the type $SiO-H \cdots A$ (A = O, N) has been studied in the gas phase for simple $H_3SiOH \cdot$acceptor complexes with the acceptor molecules being $O(H)SiH_3$, OH_2, $O(H)CH_3$, $O(CH_3)_2$, $O(CH_3)$-SiH_3, $O(SiH_3)_2$, NH_3, $N(CH_3)H_2$, $N(CH_3)_2H$, $N(CH_3)_3$, $N(CH_3)_2C_6H_5$, and NC_5H_5, respectively, at the B3LYP/6-311+(2d,p) level of theory, using Bader's atoms in molecules (AIM) and Weinhold's natural bond orbital (NBO) methodology. For all complexes (except $H_3SiOH \cdot N(CH_3)_2C_6H_5$) the complex energy $E_{add.}$ is a good estimate for the hydrogen bond energy E_{HB}, which is generally higher in N-acceptor complexes (-5.52 to -7.17 kcal mol^{-1}) than in O-acceptor complexes (-2.09 to -5.06 kcal mol^{-1}). In case of $H_3SiOH \cdot N(CH_3)_2C_6H_5$, E_{HB} and $E_{add.}$ differ by the energy associated with the loss of $n(N) \rightarrow \pi$ conjugation in $N(CH_3)_2C_6H_5$ upon complex formation. E_{HB} shows no correlation with $O \cdots A$ distances and the red shifts $\Delta\nu(OH)$ of the OH-stretching vibrations when different acceptors are compared, although both parameters are commonly used to estimate the strength of the hydrogen bond from spectroscopic and diffraction data. A good linear correlation of the hydrogen bond energy E_{HB} has been established with parameters derived from the AIM and NBO analyses, namely, the electron densities $\rho(HA)$ and $\rho(OH)$ at the $H \cdots A$ and $O-H$ bond critical points (BCPs) and the NLMO bond orders $BO_{NLMO}(HA)$ of the $H \cdots A$ bonds of the $H_3SiOH \cdot$acceptor complexes as well as the change of natural charges $\Delta q_{NPA}(O)$ at the O-donor atom upon $H_3SiOH \cdot$acceptor complex formation. Hydrogen bonding of the type $SiO-H \cdots A$ (A = O, N) has been also studied in the related cyclic multiple $H_3SiOH \cdot$acceptor complexes $(H_3SiOH)_3$, $(H_3SiOH)_2 \cdot NC_5H_5$, and $(H_3SiOH)_4$, respectively, at the same level of theory. Cooperative hydrogen bonding is evident for all cyclic multiple $H_3SiOH \cdot$acceptor complexes, whereby the strongest concomitant strengthening of the hydrogen bonds is observed for $(H_3SiOH)_4$ and $(H_3SiOH)_2 \cdot NC_5H_5$.

Introduction

Silicon and oxygen are the most abundant elements of the earth's crust and take part in ubiquitous minerals such as silicates and feldspars. The surface of these minerals as well as synthetic silica materials is covered by silanol groups that are able to bind polar molecules, such as water, alcohols, ethers, and amines *via* $SiO-H \cdots A$ hydrogen bonding (A = O, N).[1]

Chemical weathering of silicate minerals releases a steady amount of orthosilicic acid $Si(OH)_4$ into rainwater, which is carried by rivers to the oceans. Seawater typically contains 70 μM of dissolved $Si(OH)_4$, which adds up globally to 9.6 Ttons.[2] The dominant removal process of $Si(OH)_4$ is biogenic precipitation by marine microorganisms, such as diatoms, radiolarians, and sponges, estimated to cycle more than 6.7 Gtons of SiO_2 annually.[2] Diatoms exploit $Si(OH)_4$ to build up exoskeletons of amorphous silica with a wealth of different shapes and sizes. The precision at which these organisms achieve structural control has inspired material scientists to attempt biometric sol−gel silica syntheses. This silicon biomineralization process is controlled by dedicated proteins, named silicateins, which are believed to interact with $Si(OH)_4$ via $SiO-H \cdots A$ hydrogen bonding (A = O, N), whereby side chains of serine and histidine containing O and N acceptor atoms situated in the binding pocket of the proteins play important roles for the biological activity.[3]

Organosilanols, $R_nSi(OH)_{4-n}$, and alkoxysilanols, $(RO)_nSi$-$(OH)_{4-n}$ (R = alkyl, aryl), can be regarded as organic derivatives and partial esters, respectively, of orthosilicic acid, $Si(OH)_4$. Organosilanols, alkoxysilanols, and related siloxanols containing small substituents are important intermediates of the silicone polymer production and the sol−gel process.[4] Computational studies suggest that the silanol intermediates of both processes form hydrogen-bonded complexes with themselves, water, and solvent molecules prior to condensation; however, these studies have not addressed questions related to the nature of $SiO-H \cdots A$ hydrogen bonds (A = O, N).[5]

Kinetically stabilized organosilanols, alkoxysilanols, and related siloxanols resisting condensation are well-known for their self-organization in the solid state.[6] Silanols possess both excellent donor and acceptor sites for hydrogen-bonded assemblies with themselves, alcohols,[7] ethers,[8] or amines.[9] While several hydrogen bond motifs of simple silanols have been also studied computationally in the gas phase, very little is known about isolated hydrogen-bonded complexes between silanols and alternative acceptor molecules.[10] Our ambition to use polysilanols as building blocks for crystal engineering studies[11] has prompted us to investigate $SiO-H \cdots A$ hydrogen bonds (A = O, N) in simple representative $H_3SiOH \cdot$acceptor complexes with the acceptor molecules being $O(H)SiH_3$, OH_2, $O(H)CH_3$, $O(CH_3)_2$, $O(CH_3)SiH_3$, $O(SiH_3)_2$, NH_3, $N(CH_3)H_2$, $N(CH_3)_2H$, $N(CH_3)_3$, $N(CH_3)_2C_6H_5$, and NC_5H_5, respectively, by means of
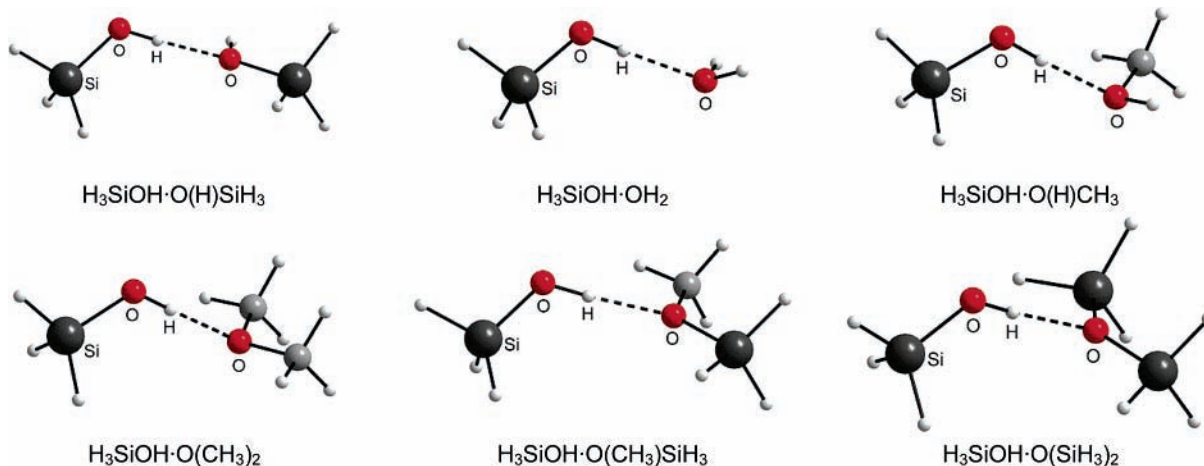
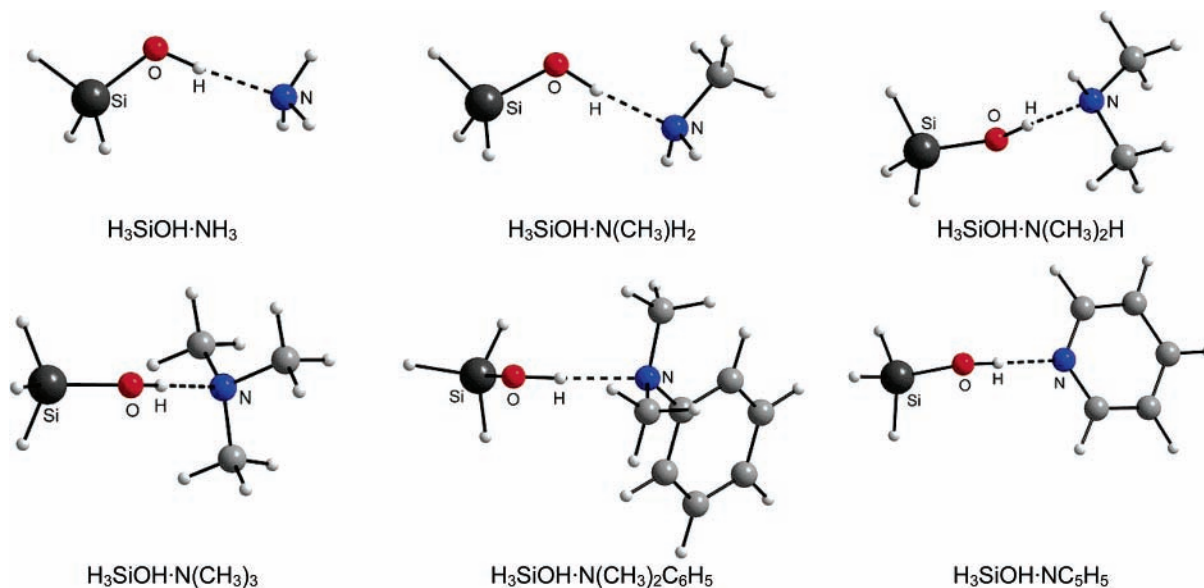**Figure 1.** Optimized gas-phase structures of simple $H_3SiOH \cdot$acceptor complexes featuring O-acceptor molecules.

Figure 2. Optimized gas-phase structures of simple $H_3SiOH \cdot$acceptor complexes featuring N-acceptor molecules.

density functional theory (DFT) calculations and topological (atoms in molecules (AIM)) and population (natural bond orbital (NBO)) analyses. The cyclic multiple $H_3SiOH \cdot$acceptor complexes $(H_3SiOH)_3$, $(H_3SiOH)_4$, and $(H_3SiOH)_2 \cdot NC_5H_5$ have been also studied to unravel possible cooperative hydrogen-bonding effects.

Computational Methodology

The geometry of the model complexes was fully optimized at the B3LYP/6-311+(2d,p) level of theory using the Gaussian W03 suite of programs.[12] It has been demonstrated that this level is sufficient to produce reliable and consistent data on small molecules with heteroatoms.[13] Frequency calculations assured that the stationary points represent minima on the potential energy surface (PES). The complex energies $E_{add.}$ have been obtained from the difference of the molecular energies of the complexes and the corresponding isolated molecules. They have been corrected for zero point vibrational energy, scaled with 0.9877,[13] and for basis set superposition error by the counterpoise procedure.[14] Wavenumbers related to the OH stretching vibrations $\nu(OH)$ have been obtained from frequency analyses and scaled by the factor 0.9679.[13] Topological analyses were performed to calculate the charge density ($\rho(OH)/\rho(HA)$) at the O−H and H···A (A = O, N) bond critical points (BCPs) and

its Laplacian ($\nabla^2\rho(OH)/\nabla^2\rho(HA)$) using Bader's atoms in molecules (AIM) theory[15] and the AIM2000 program.[16] Analyses of n(A)→σ(O−H)* negative hyperconjugation have been performed using Weinhold's natural bond orbital (NBO) theory[17] and the NBO 3.1 program[18] as implemented in Gaussian W03.
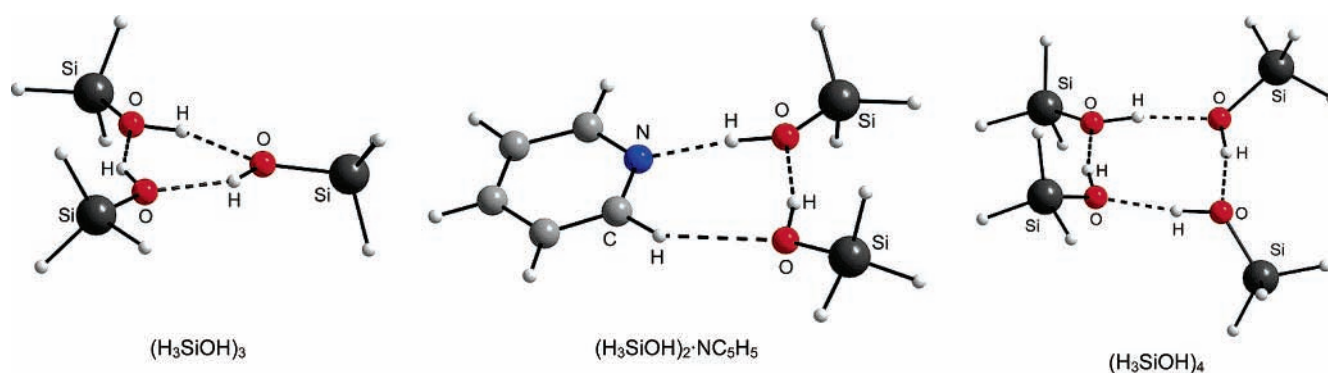
Results and Discussion

Structure and Hydrogen Bond Energies of Simple $H_3SiOH \cdot$ Acceptor Complexes. The optimized gas-phase structures of simple $H_3SiOH \cdot$acceptor complexes with acceptor molecules being $O(H)SiH_3$, OH_2, $O(H)CH_3$, $O(CH_3)_2$, $O(CH)_3SiH_3$, $O(SiH_3)_2$, NH_3, $N(CH_3)H_2$, $N(CH_3)_2H$, $N(CH_3)_3$, $N(CH_3)_2C_6H_5$, and NC_5H_5, respectively, are shown in Figures 1 and 2. The complex energies $E_{add.}$ are collected in Table 1 and fall in the range between −2.09 and −7.17 kcal mol^{-1}. The lowest energy is observed for the complex $H_3SiOH \cdot O(SiH_3)_2$, which reflects the well-known poor basicity of the siloxane linkage.[19] The second lowest $E_{add.}$ value (−3.47 kcal mol^{-1}) is observed for the complex $H_3SiOH \cdot O(H)SiH_3$, which can be regarded as a benchmark when competitive hydrogen bonding with alternative acceptors is invoked.[11] Indeed, all other complexes calculated in this work show higher $E_{add.}$ values, which is consistent with the experimental observation that organosilanols undergo complex formation with alternative acceptor molecules, such as

Supramolecular Silanol Chemistry in the Gas Phase

J. Phys. Chem. A, Vol. 111, No. 10, 2007 **2013**

TABLE 1: Complex Energy ($E_{add.}$),[a] Red Shift of the O−H Bond Stretching Vibration ($\Delta\nu$(OH)), Geometric Hydrogen Bond Parameters (Si−O, O−H, H···A, O···A, O−H−A), Electron Density (ρ(OH), ρ(HA)), and Laplacian Density ($\nabla^2\rho$(OH), $\nabla^2\rho$(HA)) of Simple H_3SiOH·Acceptor Complexes

H_3SiOH·acceptor complex	$E_{add.}$ (kcal mol^{-1})	$\Delta\nu$(OH) (cm^{-1})	Si−O (Å)	O−H (Å)	H···A (Å)	O···A (Å)	O−H−A (deg)	ρ(OH) 10^{-2} au	$\nabla^2\rho$(OH) 10^{-2} au	ρ(HA) 10^{-2} au	$\nabla^2\rho$(HA) 10^{-2} au
H_3SiOH·O(H)SiH$_3$	−3.47	195.4	1.649	0.971	1.894	2.863	176.70	34.4[c]	−58.2[c]	2.59	2.40
H_3SiOH·OH$_2$	−3.85	219.7	1.648	0.975	1.872	2.843	177.19	34.3	−58.0	2.79	2.53
H_3SiOH·O(H)CH$_3$	−4.82	277.5	1.647	0.975	1.831	2.805	176.66	34.0	−57.3	3.14	2.71
H_3SiOH·O(CH$_3$)$_2$	−5.06	300.4	1.647	0.976	1.816	2.791	178.37	33.9	−57.0	3.26	2.79
H_3SiOH·O(CH$_3$)SiH$_3$	−3.73	240.3	1.648	0.973	1.857	2.826	173.14	34.2	−57.7	2.98	2.66
H_3SiOH·O(SiH$_3$)$_2$	−2.09	157.6	1.651	0.968	1.958	2.924	176.05	34.7	−58.4	2.60	2.38
H_3SiOH·NH$_3$	−5.90	456.9	1.642	0.983	1.865	2.846	175.24	32.4	−53.5	3.57	2.28
H_3SiOH·N(CH$_3$)H$_2$	−6.92	558.5	1.641	0.988	1.824	2.809	173.84	32.1	−52.4	4.05	2.34
H_3SiOH·N(CH$_3$)$_2$H	−7.17	622.9	1.640	0.992	1.802	2.790	173.44	31.9	−51.9	4.35	2.33
H_3SiOH·N(CH$_3$)$_3$	−6.59	651.5	1.641	0.993	1.797	2.787	174.22	33.0	−54.3	4.45	2.29
H_3SiOH·N(CH$_3$)$_2$C$_6$H$_5$	−3.53 (−5.52)[b]	473.0	1.646	0.983	1.875	2.848	169.91	32.7	−54.5	3.63	2.21
H_3SiOH·NC$_5$H$_5$	−6.47	500.1	1.642	0.985	1.830	2.815	178.30	32.4	−53.5	3.86	2.39

[a] For all complexes except H_3SiOH·N(CH$_3$)$_2$C$_6$H$_5$, the complex energy $E_{add.}$ is a good estimate for the hydrogen bond energy E_{HB}. [b] Hydrogen bond energy E_{HB} estimated from electron density ρ_{HA} at the H···A BCP (see text for details). [c] Free H_3SiOH: ρ(OH), 35.80 × 10^{-2} au and $\nabla^2\rho$(OH), −58.88 × 10^{-2} au.

Figure 3. Optimized gas-phase structures and cyclic multiple H_3SiOH·acceptor complexes.

water, alcohols, ethers, and amines in the solid state.[7−9] With the exception of H_3SiOH·N(CH$_3$)$_2$C$_6$H$_5$, all N-acceptor complexes are energetically more stable than the O-acceptor complexes. In most cases, H_3SiOH and the acceptor molecules undergo only marginal changes in geometry upon complex formation, and consequently, the complex energy $E_{add.}$ can be considered as being a good estimate for the hydrogen bond energy E_{HB}. However, notable structural changes have been observed for the complexes with O(SiH$_3$)$_2$ and N(CH$_3$)$_2$C$_6$H$_5$. The Si−O−Si angle of O(SiH$_3$)$_2$ decreases by 7.6° (from 141.6 to 134.0°) upon complex formation. In comparison, the Si−O−C and C−O−C angular change in O(CH$_3$)SiH$_3$ and O(CH$_3$)$_2$ upon complex formation is only 1.4 and 0.4°, respectively. According to a single-point calculation of O(SiH$_3$)$_2$ at 134.0° (coordinates taken from the H_3SiOH·O(SiH$_3$)$_2$ complex), the angular change is associated with an energy cost of only 0.35 kcal mol^{-1}. This observation is consistent with the fact that the siloxane linkage is very flexible and the bending potential energy function is very flat for large Si−O−Si angles.[20] In turn, the angular compression of O(SiH$_3$)$_2$ upon complex formation may imply that the siloxane linkage becomes a better hydrogen bond acceptor at even smaller Si−O−Si angles; however, this idea will be examined more closely in a forthcoming paper.[21] In free N(CH$_3$)$_2$C$_6$H$_5$ the two methyl groups are nearly coplanar with the phenyl ring (torsion angle C−C−N−C, 13.7°), allowing maximum π-conjugation between these groups. In the H_3SiOH· N(CH$_3$)$_2$C$_6$H$_5$ complex, the nitrogen atom is tetrahedral and only one methyl group is nearly coplanar with the phenyl ring (torsion angle C−C−N−C, 6.3°), while the other one is twisted (torsion angle C−C−N−C, 56.8°). Apparently, in this case the hydrogen bonding is in competition with the π-conjugation,

which provides a reasonable explanation for the lower complex energy of H_3SiOH·N(CH$_3$)$_2$C$_6$H$_5$ when compared to the other N-acceptor complexes. In this case, the complex energy $E_{add.}$ is a poor estimate for the hydrogen bond energy E_{HB} as it is partly compensated by the energy loss associated with the disruption of the π-conjugation. For a better estimate of E_{HB} of H_3SiOH·N(CH$_3$)$_2$C$_6$H$_5$, see below.

Structure and Hydrogen Bond Energies of Cyclic Multiple H_3SiOH·Acceptor Complexes. The optimized gas-phase structures of cyclic multiple H_3SiOH·acceptor complexes (H_3SiOH)$_3$, (H_3SiOH)$_4$, and (H_3SiOH)$_2$·NC$_5$H$_5$ are shown in Figure 3, and related complex energies $E_{add.}$ are collected in Table 2. The complex energies $E_{add.}$ (per hydrogen bridge) of the cyclic silanol trimer (H_3SiOH)$_3$ and the cyclic silanol tetramer (H_3SiOH)$_4$ are −11.62 (−3.87) and −20.77 (−5.19) kcal mol^{-1}, respectively. Apparently, in both cyclic structures the hydrogen bonds are more stable than in the dimer H_3SiOH·O(H)SiH$_3$ (−3.47 kcal mol^{-1}), which is attributed to the concomitant strengthening of the sequential hydrogen bonds, an effect that is referred to as cooperative hydrogen bonding in the literature.[22] Similar cooperative effects have recently been established both computationally and experimentally in various water clusters.[23] The fact that (H_3SiOH)$_4$ is more stable than (H_3SiOH)$_3$ is consistent with the observation that many triorganosilanols, such as Ph$_3$-SiOH,[24] crystallize as tetramers, whereas silanol trimers have not yet been observed experimentally.[6] The complex energy $E_{add.}$ of (H_3SiOH)$_2$·NC$_5$H$_5$ (−13.12 kcal mol^{-1}) is by 3.18 kcal mol^{-1} more stable than the sum of $E_{add.}$ calculated for H_3SiOH· O(H)SiH$_3$ (−3.47 kcal mol^{-1}) and H_3SiOH·NC$_5$H$_5$ (−6.47 kcal mol^{-1}), which also points to a mutual strengthening of the sequential hydrogen bond systems, associated with cooperative

TABLE 2: Complex Energy ($E_{add.}$),[a] Red Shift of the O−H Bond Stretching Vibration ($\Delta\nu$(OH)), Geometric Hydrogen Bond Parameters (Si−O, O−H, H···A, O···A, O−H−A), Electron Density (ρ(OH), ρ(HA)), and Laplacian Density ($\triangledown^2\rho$(OH), $\triangledown^2\rho$(HA)) of Cyclic Multiple H$_3$SiOH·Acceptor Complexes

H$_3$SiOH·acceptor complex	$E_{add.}$ (kcal mol^{-1})	$\Delta\nu$(OH) (cm^{-1})	Si−O (Å)	O−H (Å)	H···A (Å)	O···A (Å)	O−H−A (deg)	ρ(OH) 10^{-2} au	$\triangledown^2\rho$(OH) 10^{-2} au	ρ(HA) 10^{-2} au	$\triangledown^2\rho$(HA) 10^{-2} au
(H$_3$SiOH)$_3$	−11.62										
SiO−H···O	−3.87		1.660	0.976	1.883	2.769	149.62	33.8	−57.4	2.70	2.51
SiO−H···O	−3.87		1.660	0.976	1.884	2.769	149.48	33.8	−57.4	2.70	2.51
SiO−H···O	−3.87		1.660	0.976	1.884	2.770	149.59	33.8	−57.3	2.70	2.51
(H$_3$SiOH)$_2$·NC$_5$H$_5$	−13.12										
SiO−H···O	(−4.68)[b]	341.7	1.648	0.978	1.806	2.765	165.65	33.4	−56.6	3.25	2.82
SiO−H···N	(−8.19)[b]	763.0	1.652	1.000	1.742	2.731	169.55	31.2	−51.0	4.84	2.44
(H$_3$SiOH)$_4$	−20.77										
SiO−H···O	−5.19		1.662	0.985	1.750	2.719	167.03	32.7	−55.3	3.75	3.06
SiO−H···O	−5.19		1.662	0.985	1.750	2.719	166.99	32.7	−55.3	3.75	3.06
SiO−H···O	−5.19		1.662	0.985	1.750	2.720	167.57	32.7	−55.3	3.75	3.06
SiO−H···O	−5.19		1.662	0.985	1.750	2.720	167.62	32.7	−55.3	3.75	3.06

[a] For (H$_3$SiOH)$_3$ and (H$_3$SiOH)$_4$, the complex energy $E_{add.}$ divided by the number of hydrogen bonds is an estimate for the hydrogen bond energy E_{HB}. [b] Hydrogen bond energies estimated from electron densities ρ(HA) at the H···A BCP (see text for details).

effects. For the estimate of individual SiO−H···N and SiO−H···O(H)Si E_{HB} of (H$_3$SiOH)$_3$, (H$_3$SiOH)$_4$, and (H$_3$SiOH)$_2$·NC$_5$H$_5$, see below.

Geometric Hydrogen Bond Parameters. The hydrogen bond parameters of the simple H$_3$SiOH·acceptor complexes and the cyclic multiple H$_3$SiOH·acceptor complexes are collected in Tables 1 and 2. The reference Si−O and O−H bond lengths calculated for isolated H$_3$SiOH are 1.660 and 0.960 Å, respectively. As expected, the Si−O bond length of H$_3$SiOH decreases marginally upon complex formation within all acceptor molecules. For the simple H$_3$SiOH·acceptor complexes the largest decrease being 0.020 Å is observed for one of the strongest complexes, namely, the H$_3$SiOH·N(CH$_3$)$_2$H complex. In turn, the O−H bond length slightly increases upon complex formation with a maximum of 0.033 Å being observed for the strong complex H$_3$SiOH·N(CH$_3$)$_3$. The O···O and O···N distances of the simple H$_3$SiOH·acceptor complexes vary between 2.924 (O(SiH$_3$)$_2$) and 2.787 Å (N(CH$_3$)$_3$), which is consistent with medium strength hydrogen bonding.[22] As the exact localization of hydrogen atoms by X-ray diffraction is usually difficult, the donor···acceptor distance is often the only geometric parameter used to evaluate the strength of hydrogen bonds.[6] In light of this practice it is important to note that only a very poor correlation exists between $E_{add.}$ and the donor···acceptor distance when *different* acceptor types are compared. For instance, the O···A distances of H$_3$SiOH·O(H)SiH$_3$ (2.863 Å) and H$_3$SiOH·NC$_5$H$_5$ (2.815 Å) differ only by 1.6%, whereas $E_{add.}$ (−3.47 and −6.47 kcal mol^{-1}) vary by 46%. For the evaluation of E_{HB} of complexes containing *different* acceptor types, the Si−O bond length seems to be a more suitable geometric parameter. The graphical correlation and linear regression data of $E_{add.}$ vs the Si−O bond lengths for the simple H$_3$SiOH·acceptor complexes except H$_3$SiOH·N(CH$_3$)$_2$C$_6$H$_5$ are shown in Figure 4. Unfortunately, the Si−O bond lengths determined by X-ray diffraction are usually affected by errors that are too large for the precise determination of hydrogen bond energies.[6] The donor···acceptor distance of complexes that contain the *same* acceptor may be correlated in terms of their hydrogen bond energies. Thus, the O···O distance of the tetramer (H$_3$SiO)$_4$ (average 2.7195 Å) is by 0.144 Å shorter than in the dimer H$_3$SiOH·O(H)SiH$_3$ (2.863 Å), for which also the smaller $E_{add.}$ has been observed.

Red Shift of the OH Stretching Vibrations. It is common practice to establish the hydrogen bond strengths of silanols by IR and less often by Raman spectroscopy.[6] Usually, the OH stretching vibration ν(OH) of the silanol undergoes an indicative
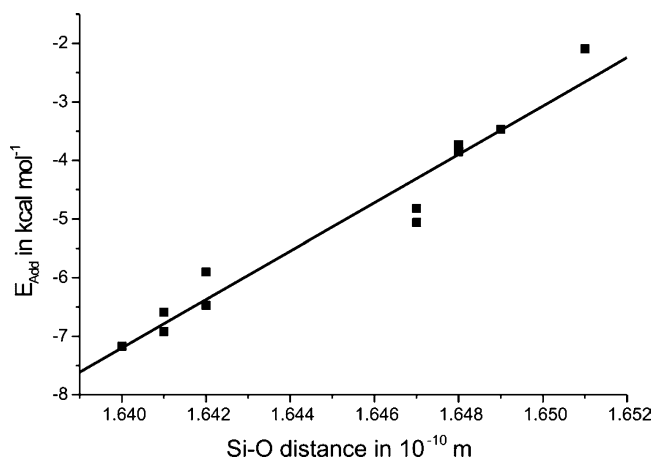

Figure 4. Correlation of the complex energy $E_{add.}$ vs the Si−O bond lengths for the simple H$_3$SiOH·acceptor complexes (except H$_3$SiOH·N(CH$_3$)$_2$C$_6$H$_5$). Linear regression: $E_{add.} = [413 \pm 33$ kcal/(mol 10^{-10} m)]·d(Si−O) − [684 ± 53 kcal/mol]; $R = 0.97$.

red shift upon complex formation, which has been used as spectroscopic probe for the determination of E_{HB}. The frequency analysis of the free H$_3$SiOH molecule reveals that an OH stretching vibration ν(OH) occurs at 3766.7 cm^{-1}, which is consistent with experimental values of isolated silanol groups.[25] In all H$_3$SiOH·acceptor complexes, the OH stretching vibrations ν(OH) are red-shifted. The vibrational red shifts $\Delta\nu$(OH) of the simple H$_3$SiOH·acceptor complexes are collected in Table 1 and range from 157.6 (H$_3$SiOH·O(SiH$_3$)$_2$) to 651.5 cm^{-1} (H$_3$SiOH···N(CH$_3$)$_3$). Although there is a general trend that with an increasing $E_{add.}$ the vibrational red shift $\Delta\nu$(OH) will be also larger, only the O-acceptors exhibit a linear correlation. The graphical correlation and linear regression data of $E_{add.}$ vs $\Delta\nu$-(OH) for the simple H$_3$SiOH·O-acceptor complexes are shown in Figure 5. The cyclic trimer (H$_3$SiOH)$_3$ shows two asymmetric and one symmetric coupled OH stretching vibrations, which are red-shifted by 262.4, 262.5, and 320.0 cm^{-1}, respectively. The cyclic tetramer (H$_3$SiOH)$_4$ reveals three asymmetric and one symmetric coupled OH stretching vibrations that are red-shifted by 413.2, 448.1, 449.0, and 537.5 cm^{-1}, respectively. The red shifts of (H$_3$SiOH)$_3$ and (H$_3$SiOH)$_4$ are larger than that of the simple complex H$_3$SiOH·O(H)SiH$_3$ (195.4 cm^{-1}), which is consistent with the trend observed with the E_{HB} values. For (H$_3$SiOH)$_2$·NC$_5$H$_5$, $\Delta\nu$(OH) of 341.7 SiO−H···O and 763.0 cm^{-1} (SiO−H···N) are larger than those calculated for the simple complexes H$_3$SiOH·O(SiH$_3$)H (195.4 cm^{-1}) and H$_3$SiOH·NC$_5$H$_5$ (195.4 cm^{-1}), respectively, indicating that the

Supramolecular Silanol Chemistry in the Gas Phase
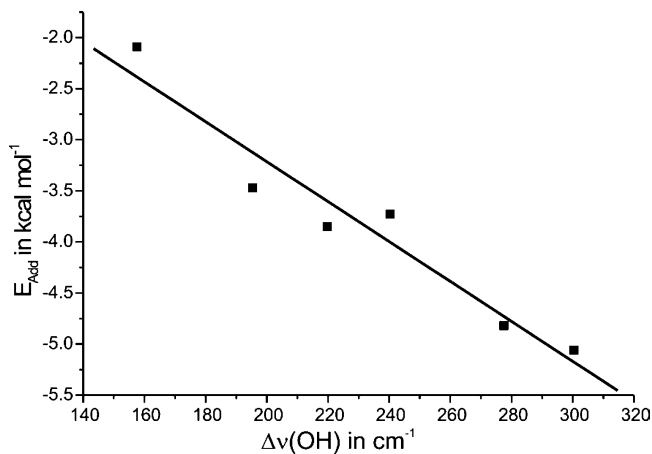
J. Phys. Chem. A, Vol. 111, No. 10, 2007 **2015**

Figure 5. Correlation of the complex energy $E_{add.}$ vs the red shift of the OH stretching vibration $\Delta\nu(OH)$ for simple $H_3SiOH \cdot \Delta\nu(OH)$ acceptor complexes. Linear regression: $E_{add.} = [-0.019 \pm 0.002$ kcal cm/mol$] + [0.7 \pm 0.6$ kcal/mol$]$; $R = 0.97$.

Figure 6. Correlation of the complex energy $E_{add.}$ vs electron density at the H···A bond critical point $\rho(HA)$ for all model complexes (except $H_3SiOH \cdot N(CH_3)_2C_6H_5$ and $H_3SiOH \cdot NC_5H_5$. Linear regression: $E_{add.} = [-220.8 \pm 24.9$ kcal/(mol au)$] \cdot \rho(HA) + [2.5 \pm 0.9$ kcal/mol$]$; $R = 0.94$.

Figure 7. Correlation of the complex energy $E_{add.}$ vs electron density at the O−H bond critical point $\rho(OH)$ for all model complexes (except $H_3SiOH \cdot N(CH_3)_2C_6H_5$ and $H_3SiOH \cdot NC_5H_5$. Linear regression: $E_{add.} = [146 \pm 19$ kcal/(mol au)$] \cdot \rho(OH) - [54 \pm 6$ kcal/mol$]$; $R = 0.92$.

sequential hydrogen bridge is stronger than the sum of the isolated hydrogen bonds. It is worth mentioning that experimentally observed OH stretching vibrations $\nu(OH)$ are usually very broad. In complex systems the vibrations inevitably overlap, precluding the reliable interpretation of this parameter.

AIM Analyses. Recently, Bader's AIM theory has been applied very successfully for topological analyses of the electron density of hydrogen bond complexes.[26] According to the AIM theory, the formation of a O−H···A hydrogen bond is associated with the appearance of a bond path between the hydrogen and the acceptor atom and the occurrence of a bond critical point (BCP) along this path. The H···A BCP of hydrogen bonds has typical properties of a closed-shell interaction. The value of the charge density $\rho(HA)$ is comparatively low and the Laplacian of the charge density $\nabla^2\rho(HA)$ is positive, indicating that the interaction is dominated by the construction of charge away from the interatomic surface toward the hydrogen and acceptor atoms. In turn, the value of $\rho(OH)$ at the O−H BCP is relatively large and $\nabla^2\rho(OH)$ is negative, showing that the electronic charge is concentrated in the internuclear region. Eight topological criteria defining a hydrogen bond have been proposed, two of which entail that $\rho(HA)$ and $\nabla^2\rho(HA)$ should lie between 0.2×10^{-2} and 3.5×10^{-2} au and 2.4×10^{-2} and 13.9×10^{-2} au, respectively.[26] The electron densities ($\rho(OH)/\rho(HA)$) and their Laplacians ($\nabla^2\rho(OH)/\nabla^2\rho(HA)$) at the O−H and H···A BCPs of the simple $H_3SiOH \cdot$acceptor complexes are collected in Table 1. $\rho(HA)$ and $-^2\rho(HA)$ at the H···A BCP fall in the range from 2.59×10^{-2} ($H_3SiOH \cdot O(H)SiH_3$ to 4.45×10^{-2} au ($H_3SiOH \cdot N(CH_3)_3$) and from 2.21×10^{-2} ($H_3SiOH \cdot N(CH_3)_2C_6H_5$) to 2.79×10^{-2} au ($H_3SiOH \cdot O(CH_3)_2$), respectively. Thus, $\rho(HA)$ are at the upper limit or slightly above the definition range, whereas $\nabla^2\rho(HA)$ are at the lower limit or even slightly below. Apparently, the hydrogen bonds discussed in this work have a higher covalent bond character than the reference complexes reported in the literature.[26] $\rho(OH)$ and $\nabla^2\rho(OH)$ at the O−H BCP of free H_3SiOH adopt values of 35.80×10^{-2} and -58.88×10^{-2} au, respectively. Upon complex formation, $\rho(OH)$ slightly decreases to values between 34.7×10^{-2} ($H_3SiOH \cdot O(SiH_3)_2$) and 31.9×10^{-2} au ($H_3SiOH \cdot N(CH_3)_2H$), whereas $\nabla^2\rho(OH)$ increases to values between -58.4×10^{-2} ($H_3SiOH \cdot O(SiH_3)_2$) and -51.9×10^{-2} au ($H_3SiOH \cdot N(CH_3)_2H$), which is consistent with a decrease of the O−H covalent bond character and an increase of charge separation, so that the oxygen atom becomes more negative and the hydrogen atom becomes more positive.
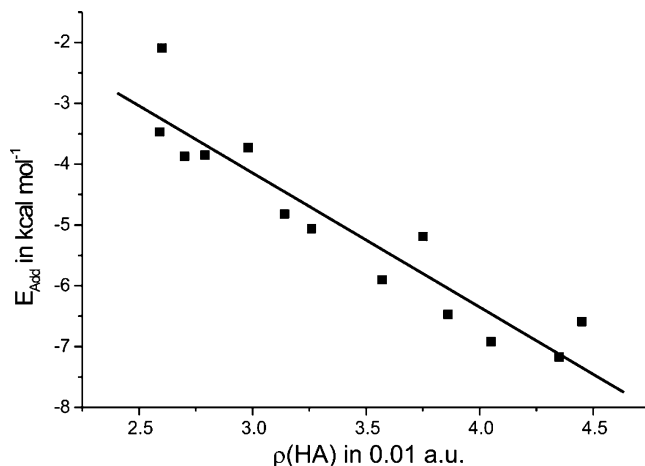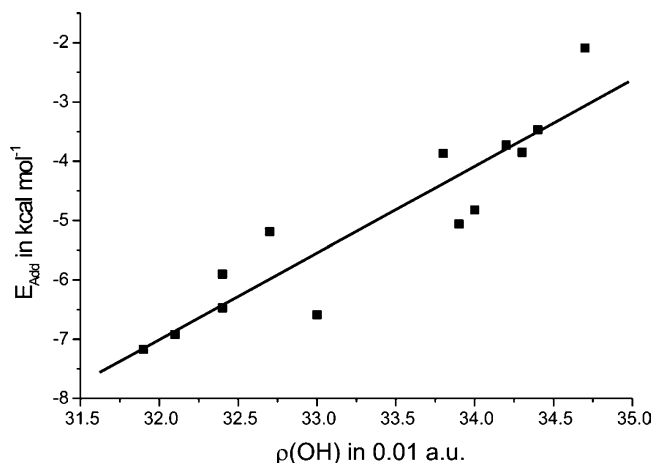
$\rho(OH)/\rho(HA)$ and $\nabla^2\rho(OH)/\nabla^2\rho(HA)$ at the O−H and H···A BCPs of the cyclic multiple $H_3SiOH \cdot$acceptor complexes are collected in Table 2. The graphical correlation and linear regression data of $E_{add.}$ vs $\rho(OH)$ and $\rho(HA)$ at the O−H and H···A BCPs of all model complexes except $H_3SiOH \cdot N(CH_3)_2C_6H_5$ and $(H_3SiOH)_2 \cdot NC_5H_5$ are shown in Figures 6 and 7. E_{HB} of $H_3SiOH \cdot N(CH_3)_2C_6H_5$ estimated using the regression curve $E_{add.}$ vs $\rho(HA)$ is -5.52 kcal mol^{-1}, which compares well with $E_{add.}$ of the other $H_3SiOH \cdot$N-acceptor complexes (Table 1) and indeed confirms that the loss of π-conjugation lowers $E_{add.}$ of $H_3SiOH \cdot N(CH_3)_2C_6H_5$ (-3.53 kcal mol^{-1}). When the same approach is applied to cyclic multiple complex $(H_3SiOH)_2 \cdot NC_5H_5$, the SiO−H···O and SiO−H···N E_{HB} are estimated at -4.68 and -8.19 kcal mol^{-1}, respectively. The sum of these two E_{HB} (-12.87 kcal mol^{-1}) almost matches $E_{add.}$ of $(H_3SiOH)_2 \cdot NC_5H_5$ (-13.12 kcal mol^{-1}). Having established these hydrogen bond energy values, a comparison with the complex energies of the simple model complexes $H_3SiOH \cdot O(H)SiH_3$ (-3.47 kcal mol^{-1}) and $H_3SiOH \cdot NC_5H_5$ (-6.47 kcal mol^{-1}) reveals a concomitant strengthening of the SiO−H···O and SiO−H···N hydrogen bonds in the cyclic multiple $H_3SiOH \cdot$acceptor complexes approximately by 1.36 and 1.69 kcal mol^{-1}, which is consistent with the idea of cooperative hydrogen bonding. Recently, we have prepared a

TABLE 3: Natural Charge at the Acceptor Atom (q_{NPA}(A)) of the Free Acceptor Molecule and Natural Charge Transfer[a] (Δq_{NPA}) at A, H, O, and Si upon Complex Formation of Simple H₃SiOH·Acceptor Complexes

H₃SiOH·acceptor complex	q_{NPA}(A) (e)	Δq_{NPA}(A) (e)	Δq_{NPA}(H) (e)	Δq_{NPA}(O) (e)	Δq_{NPA}(Si) (e)
H₃SiOH·O(H)SiH₃	−1.089	−0.022	0.023	−0.023	0.009
H₃SiOH·OH₂	−0.936	−0.015	0.023	−0.028	0.010
H₃SiOH·O(H)CH₃	−0.757	−0.021	0.021	−0.030	0.010
H₃SiOH·O(CH₃)₂	−0.615	−0.018	0.018	−0.029	0.009
H₃SiOH·O(CH₃)SiH₃	−0.925	−0.025	0.022	−0.026	0.008
H₃SiOH·O(SiH₃)₂	−1.251	−0.014	0.019	−0.018	0.006
H₃SiOH·NH₃	−1.063	−0.010	0.025	−0.042	0.011
H₃SiOH·N(CH₃)H₂	−0.863	−0.013	0.021	−0.045	0.011
H₃SiOH·N(CH₃)₂H	−0.702	−0.021	0.019	−0.045	0.010
H₃SiOH·N(CH₃)₃	−0.589	−0.026	0.014	−0.043	0.010
H₃SiOH·N(CH₃)₂C₆H₅	−0.566	−0.066	0.013	−0.034	0.010
H₃SiOH·NC₅H₅	−0.507	−0.049	0.023	−0.040	0.013

[a] $\Delta q < 0$, charge transfer to the atom; $\Delta q > 0$, charge transfer from the atom.

TABLE 4: Natural Charge Transfer[a] (Δq_{NPA}) at A, H, O, and Si upon Complex Formation of Cyclic Multiple H₃SiOH·Acceptor Complexes

H₃SiOH·acceptor complex	Δq_{NPA}(A) (e)	Δq_{NPA}(H) (e)	Δq_{NPA}(O) (e)	Δq_{NPA}(Si) (e)
(H₃SiOH)₃				
SiO−H···O	−0.054	0.038	−0.054	0.009
SiO−H···O	−0.054	0.038	−0.054	0.009
SiO−H···O	−0.054	0.038	−0.054	0.009
(H₃SiOH)₂·NC₅H₅				
SiO−H···O	−0.072	0.033	−0.043	0.013
SiO−H···N	−0.059	0.032	−0.072	0.012
(H₃SiOH)₄				
SiO−H···O	−0.059	0.092	−0.059	0.006
SiO−H···O	−0.058	0.092	−0.058	0.006
SiO−H···O	−0.058	0.093	−0.058	0.007
SiO−H···O	−0.057	0.093	−0.057	0.007

[a] $\Delta q < 0$, charge transfer to the atom; $\Delta q > 0$, charge transfer from the atom.

number of self-assembled 1:1 complexes of the trisilanol 1,3,5-(HO*i*-Pr₂Si)₃C₆H₃ and various 4,4′-bis(pyridines), which give rise to the formation of supramolecular 2D brick wall structures.[11] These structures comprise sequential hydrogen bonds of the type SiO−H···O(Si)-H···N, which are more stable than elusive 2:3 complexes having isolated SiO−H···N hydrogen bonds. Apparently, the stability of these 2D solid-state structures also relies on cooperative effects.

NBO Analyses. Negative hyperconjugation of the type n(A)→σ(O−H)* has been invoked as the main contribution to the hydrogen bond energy, which has been quantitatively assessed by NBO analyses.[27] Natural bond orbitals can be regarded as one of a sequence of natural localized orbital sets that include natural atomic (NAO), hybrid (NHO), and (semi-)localized molecular orbital (NLMO) sets, intermediate between basis AOs and canonical molecular orbitals (MOs): AOs → NAOs → NHOs → NBOs → NLMOS → MOS. These natural localized sets are complete and orthonormal and describe exactly any property of the wavefunction. Negative hyperconjugation of the type n(A)→σ(O−H)* may be associated with a transfer of natural charges q_{NPA} at the atoms in the hydrogen bridge. q_{NPA} of the free acceptor molecules and the transfer of natural charges Δq_{NPA} upon complex formation are collected for simple H₃SiOH·acceptor complexes and the cyclic multiple H₃SiOH·acceptor complexes in Tables 3 and 4, respectively. The largest q_{NPA}(A) is located at the oxygen atom of O(SiH₃)₂ (−1.251 e) due to the large electronegativity difference of Si and O and the partly ionic nature of the siloxane linkage,[28] whereas the smallest q_{NPA}(A) value is observed for NC₅H₅ (−0.507 e). Given that $E_{add.}$ of H₃SiOH·O(SiH₃)₂ (−2.09 kcal mol⁻¹) and H₃SiOH·NC₅H₅ (−6.47 kcal mol⁻¹) show a reverse trend, a large q_{NPA}(A) at the acceptor molecule is not essential for a stable

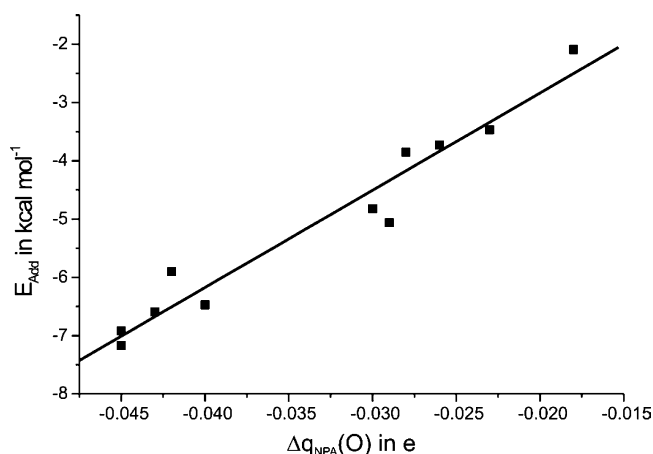**Figure 8.** Correlation of the complex energy $E_{add.}$ vs natural charge transfer at the donor oxygen atom Δq_{NPA}(O) for all model complexes. Linear regression: $E_{add.} = [167 \pm 13 \text{ kcal/(mol e)}] \cdot \Delta q_{NPA} + [0.5 \pm 0.5 \text{ kcal/mol}]$; $R = 0.97$.

hydrogen bridge. Upon H₃SiOH·acceptor complex formation, a natural charge separation occurs, whereby both the donor oxygen atom and the acceptor atom become more negative, Δq_{NPA}(O,A) < 0, whereas the hydrogen and silicon atom become more positive, Δq_{NPA}(H,Si) > 0. For the simple H₃SiOH·acceptor complexes the $E_{add.}$ values correlate well with the Δq_{NPA}(O), while all other Δq_{NPA} values lack such correlation. The graphical correlation and linear regression data of $E_{add.}$ vs Δq_{NPA}(O) are shown in Figure 8. The natural charge separation is more pronounced in the cyclic multiple H₃SiOH·acceptor complexes, which is consistent with the idea that cooperative hydrogen bonding is operative. In an attempt to

Supramolecular Silanol Chemistry in the Gas Phase

J. Phys. Chem. A, Vol. 111, No. 10, 2007 **2017**

TABLE 5: Delocalization Energy (ΔE_deloc), NBO Occupancy of σ*(OH) and n(A) Orbitals (Including the s-Character of These Orbitals) and NLMO O−H and H···A Bond Orders (BO_NLMO) of Simple H₃SiOH·Acceptor Complexes as Well as NBO Occupancy Changes[a] of σ*(OH) and n(A) Orbitals (Including the Change of s-Character of These Orbitals) upon Complex Formation

complexes	ΔE_{deloc} (kcal mol^{-1})	$N(\sigma*(OH))$ (e) (s-character of O bond hybrid (%))	$N(n(A))$ (e) (s-chara cter [%])	$\Delta N(\sigma*(OH))$ (e) (Δ s-character of O bond hybrid (%))[b]	$\Delta N(n(A))$ (e) (Δ s-character (%))	BO_NLMO (OH)	BO_NLMO (HA)
H₃SiOH·O(H)SiH₃	9.16	0.020 05 (25.2)	1.953 43 (18.6)	0.015 95 (2.9)	−0.006 97 (2.4)	0.4603	0.0135
H₃SiOH·OH₂	10.40	0.023 70 (25.4)	1.986 65 (26.1)	0.019 60 (3.1)	−0.012 69 (-0.6)	0.4569	0.0167
H₃SiOH·O(H)CH₃	12.34	0.029 08 (25.7)	1.962 80 (24.8)	0.024 98 (3.4)	−0.009 21 (-0.3)	0.4524	0.0220
H₃SiOH·O(CH₃)₂	11.62	0.031 24 (25.8)	1.944 23 (19.8)	0.027 14 (3.5)	−0.012 35 (-2.0)	0.4516	0.0231
H₃SiOH·O(CH₃)SiH₃	9.46	0.023 43 (25.4)	1.927 59 (16.7)	0.019 33 (3.1)	−0.009 37 (0.3)	0.4561	0.0145
H₃SiOH·O(SiH₃)₂	6.92	0.016 67 (24.9)	1.922 42 (10.5)	0.012 57 (2.6)	0.004 36 (2.4)	0.4677	0.0108
H₃SiOH·NH₃	18.62	0.044 66 (27.0)	1.952 65 (22.9)	0.040 56 (4.7)	−0.044 4 (4.4)	0.4332	0.0342
H₃SiOH·N(CH₃)H₂	19.49	0.051 68 (27.4)	1.918 77 (21.0)	0.047 58 (5.1)	−0.044 0 (1.0)	0.4284	0.0404
H₃SiOH·N(CH₃)₂H	19.00	0.054 53 (27.6)	1.883 92 (18.4)	0.050 43 (5.3)	−0.034 4 (1.4)	0.4269	0.0422
H₃SiOH·N(CH₃)₃	16.48	0.053 14 (27.5)	1.854 87 (15.5)	0.049 04 (5.2)	−0.022 6 (0.8)	0.4282	0.0427
H₃SiOH·N(CH₃)₂C₆H₅	11.45	0.043 31 (35.9)	1.814 78 (11.1)	0.039 21 (13.6)	0.063 75 (7.9)	0.4405	0.0259
H₃SiOH·NC₅H₅	17.89	0.051 99 (38.1)	1.888 95 (27.5)	0.047 89 (15.8)	−0.030 16 (-1.0)	0.4241	0.0354

[a] $\Delta N < 0$, decrease of orbital population; $\Delta N > 0$, increase of orbital population. [b] Free H₃SiOH: $N(\sigma*(OH))$ [0.004 10 e]; s-character of O bond hybrid [22.3%]).

TABLE 6: Delocalization Energy (ΔE_deloc), NBO Occupancy of σ*(OH) and n(A) Orbitals (Including the s-Character of These Orbitals) and NLMO O−H and H···A Bond Orders (BO_NLMO) of Cyclic Multipe H₃SiOH·Acceptor Complexes as Well as NBO Occupancy Changes[a] of σ*(OH) and n(A) Orbitals (Including the Change of s-Character of These Orbitals) upon Complex Formation

complex	ΔE_{deloc} (kcal mol^{-1})	$N(\sigma*(OH))$ (e) (s-character of O bond hybrid (%))	$N(n(A))$ (e) (s-character (%))	$\Delta N(\sigma*(OH))$ (e) (Δ s-character of O bond hybrid (%))	$\Delta N(n(A))$ (e) (Δ s-character (%))	BO_NLMO (OH)	BO_NLMO (HA)
(H₃SiOH)₃							
SiO−H···O	8.12	0.0218 3 (25.5)	1.948 51 (17.1)	0.017 73 (3.2)	−0.008 87 (−1.6)	0.4432	0.0157
SiO−H···O	7.98	0.021 80 (25.5)	1.948 50 (17.1)	0.017 70 (3.2)	−0.012 20 (−1.9)	0.4431	0.0156
SiO−H···O	8.02	0.021 85 (25.5)	1.948 47 (17.4)	0.017 75 (3.2)	−0.012 26 (−1.3)	0.4431	0.0157
(H₃SiOH)₂·C₅H₅N							
SiO−H···O	14.63	0.035 02 (36.4)	1.851 95 (19.6)	0.030 92 (14.1)	−0.102 65 (1.0)	0.4338	0.0195
SiO−H···N	26.33	0.073 70 (41.1)	1.874 21 (27.3)	0.069 6 (18.8)	−0.044 90 (−1.2)	0.3917	0.0136
(H₃SiOH)₄							
SiO−H···O	17.79	0.036 87 (26.8)	1.941 00 (16.9)	0.032 77 (4.5)	−0.013 60 (−1.8)	0.4233	0.0257
SiO−H···O	17.88	0.037 03 (26.7)	1.940 92 (16.9)	0.032 93 (4.4)	−0.013 68 (−1.8)	0.4236	0.0254
SiO−H···O	17.76	0.036 72 (26.7)	1.941 06 (16.9)	0.032 62 (4.4)	−0.013 54 (−1.8)	0.4234	0.0251
SiO−H···O	17.97	0.037 29 (26.7)	1.940 82 (17.0)	0.033 19 (4.4)	−0.013 78 (−1.7)	0.4232	0.0259

[a] $\Delta N < 0$, decrease of orbital population; $\Delta N > 0$, increase of orbital population.

quantify the degree of negative hyperconjugation of the type n(A)→σ(O−H)*, the delocalization energies ΔE_{deloc} and the NBO population of n(A) and σ(O−H)* have been calculated and listed for simple H₃SiOH·acceptor complexes and cyclic multiple H₃SiOH·acceptor complexes in Tables 5 and 6. ΔE_{deloc} follow a trend very similar to $E_{add.}$. Among the simple H₃SiOH·acceptor complexes the lowest and the highest ΔE_{deloc} values are observed for O(SiH₃)₂ (−6.92 kcal mol^{-1}) and N(CH₃)H₂ (−19.49 kcal mol^{-1}), respectively. Like those observed for water clusters with an increasing number of molecules,[23] the ΔE_{deloc} values related to the SiO−H···O bridge of the cyclic multiple H₃SiOH·acceptor complexes (H₃SiOH)₄ (−17.76 to −17.97 kcal mol^{-1}) and (H₃SiOH)₂·NC₅H₅ (−14.63 kcal mol^{-1}) are much higher than those of (H₃SiOH)₃ (−7.98 to −8.12 kcal mol^{-1}) and H₃SiOH·O(H)SiH₃ (−9.16 kcal mol^{-1}). Similarly, the ΔE_{deloc} value associated with the SiO−H···N bridge of (H₃SiOH)₂·NC₅H₅ (−26.33 kcal mol^{-1}) is much higher than in the simple complex H₃SiOH·NC₅H₅ (−17.89 kcal mol^{-1}). The observation of increasing ΔE_{deloc} of the cyclic multiple H₃SiOH·acceptor complexes (H₃SiOH)₄ and (H₃SiOH)₂·NC₅H₅ is consistent with the idea of cooperative hydrogen bonding. The NBO analysis reveals that electron density is indeed transferred from the n(A) orbital to the σ(O−H)* orbital. The highest and lowest occupancies of the σ(O−H)* orbitals are observed in the SiO−H···N bridge of (H₃SiOH)₂·NC₅H₅ (0.07370 e) and in (H₃-
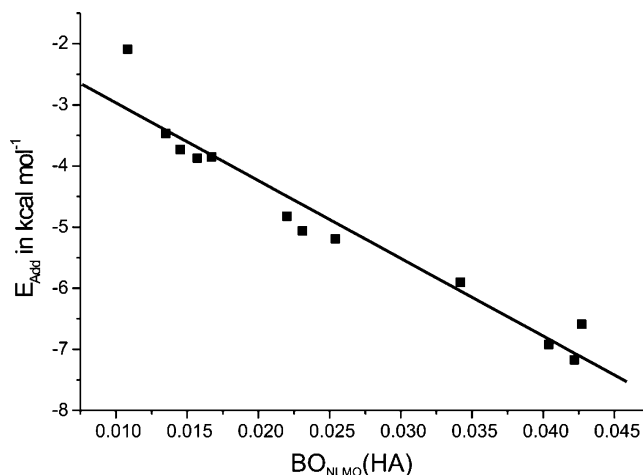

Figure 9. Correlation of the complex energy $E_{add.}$ vs NLMO bond orders BO_NLMO(HA) of the H···A bonds of all model complexes except those with aromatic acceptor molecules. Linear regression: $E_{add.} = [−130 \pm 10 \text{ kcal/mol e}] \cdot BO(HA) −[1.7 \pm 0.3 \text{ kcal/mol}]$; $R = 0.97$.

SiOH)·O(SiH₃)₂ (0.01667 e), respectively, which agrees well with the established trend of E_{HB} and ΔE_{deloc}. Of the cyclic multiple H₃SiOH·acceptor complexes (H₃SiOH)₄ and (H₃-SiOH)₂·NC₅H₅ of which cooperative hydrogen bonding is evident, the transfer of electron density into the σ(O−H)*

orbitals is more pronounced than in the simple complexes (H_3-SiOH)·O(H)SiH$_3$ and H_3SiOH·NC$_5$H$_5$. In an effort to further quantify the degree of the covalent bonding character in hydrogen bridges, NLMO bond orders BO$_{NLMO}$(OH) and BO$_{NLMO}$(HA) have been calculated for the simple H$_3$SiOH· acceptor complexes and the cyclic multiple H$_3$SiOH·acceptor complexes and are collected in Tables 5 and 6, respectively. The highest BO$_{NLMO}$(OH) of 0.4677 and lowest BO$_{NLMO}$(HA) of 0.0108 are observed in the weakest complex H$_3$SiOH· O(SiH$_3$)$_2$, having the most asymmetric O$-$H$\cdots$A hydrogen bridge. The lowest BO$_{NLMO}$(OH) of 0.4241 and the highest BO$_{NLMO}$(HA) of 0.0427 are found for two of the strongest complexes, namely, H$_3$SiOH·NC$_5$H$_5$ and H$_3$SiOH·N(CH$_3$)$_3$. A good correlation of $E_{add.}$ and BO$_{NLMO}$(HA) has been established. The graphical correlation and linear regression data of $E_{add.}$ vs BO$_{NLMO}$(HA) are shown for all complexes (except the unsaturated complexes) in Figure 9.

Conclusion

Hydrogen bonding of the type SiO$-$H$\cdots$A (A = O, N) has been studied computationally by DFT methods and AIM and NBO analyses for simple and cyclic multiple H$_3$SiOH·acceptor complexes. The hydrogen bond energies E_{HB} of N-acceptor complexes are generally higher than those of O-acceptor complexes even though this is not reflected in the donor$\cdots$ acceptor distances, which are quite similar. Cooperative hydrogen bonding has been observed for the cyclic multiple H$_3$SiOH· acceptor complexes (H$_3$SiOH)$_3$, (H$_3$SiOH)$_2$·NC$_5$H$_5$, and (H$_3$SiOH)$_4$, whereby the strongest mutual strengthening is observed in the latter two compounds. The trends of E_{HB} correlate well with experimentally established solid-state structures of silanols. For instance, the cyclic tetramers of triorganosilanols (R$_3$SiOH)$_4$ (e.g., R = Ph) are frequently observed, whereas cyclic trimers are hitherto unknown.[6,24] Cooperative effects may also explain the exclusive formation of 1:1 supramolecular complexes of the trisilanol 1,3,5-(HOi-Pr$_2$Si)$_3$C$_6$H$_3$ and various 4,4′-bis(pyridines).[11] These 1:1 cocrystals contain sequential SiO$-$H$\cdots$O(Si)-H$\cdots$N hydrogen bonds, which are apparently more stable than the isolated SiO$-$H$\cdots$N hydrogen bonds expected for the elusive 2:3 complexes. Notably, however, the absolute E_{HB} may be affected by errors related to the accuracy of the calculation. For instance, the counterpoise procedure may overestimate the BSSE.[29] The Si$-$O bond lengths seem to be a suitable geometric parameter to evaluate the hydrogen bond strength even if *different* acceptor types are compared. However, the frequently used donor$\cdots$acceptor distance only shows a very poor correlation with the hydrogen bond energy. In addition, the red shift of the OH stretching vibration $\Delta\nu$(OH) shows no general correlation with E_{HB} but may be consulted when the same acceptor type is compared in different complexes. According to the topological criteria of the AIM methodology, the hydrogen bonds examined herein are stronger and have an even more covalent character than conventional hydrogen bonds.[26] The electron densities ρ(OH) and ρ(HA) of the O$-$H and H$\cdots$A bond critical points (BCPs) correlate very well with E_{HB}. These correlations render possible the calculation of E_{HB} for complexes whose $E_{add.}$ do not coincide with their hydrogen bond energies as significant structural changes occur upon complex formation. The same procedure is also applicable for cyclic multiple H$_3$SiOH·acceptor complexes having *different* types of hydrogen bonds, such as (H$_3$-SiOH)$_2$·NC$_5$H$_5$. Natural population analyses reveal that the strength of E_{HB} are independent from the natural charges q_{NPA} of the acceptor atoms. A more significant parameter is the

natural charge transfer to the oxygen atom Δq_{NPA}(O) that occurs upon complex formation. NBO analyses further reveal that negative hyperconjugation of the type n(A)$\rightarrow\sigma$(O$-$H)*, i.e. electron population and charge transfer from the lone pair of the acceptor atom into the antibonding σ-orbital of the O$-$H bond, is operative in all hydrogen bonds. Due to the electron and charge transfer, the acceptor atom becomes more negative, whereas the hydrogen atoms become more positive. The delocalization energy ΔE_{deloc} being associated with the negative hyperconjugation follows a trend similar to E_{HB}. Bond orders of the O$-$H and H$\cdots$A bonds, BO$_{NMLO}$(OH) and BO$_{NMLO}$(HA), derived from NLMO analyses reveal also a very good correlation with E_{HB}. On the basis of the results described herein, further experimental and computational studies on silanol$\cdots$acceptor complexes are currently being undertaken.[21]

References and Notes

(1) Iler, R. K. *The Chemistry of Silica*; Wiley: New York, 1979.
(2) (a) Treguer, P.; Nelson, D. M.; Van Bennekom, A. J.; DeMaster, D. J.; Leynaert, A.; Queguiner, B. *Science* **1995**, *268*, 375−379. (b) Knight, C. T. G.; Kinrade, S. D. A Primer on the Aqueous Chemistry of Silicon. In *Silicon in Agriculture*; Datnoff, L. E., Snyder, G. H., Kinrade, S. D., Eds.; Elsevier: Amsterdam, 2001.
(3) (a) Hildebrand, M.; Volcani, B. E.; Gassmann, W.; Schröder, J. I. *Nature* **1997**, *385*, 688−689. (b) Kröger, N.; Lehmann, G.; Rachel, R.; Sumper, M. *Eur. J. Biochem.* **1997**, *250*, 99−105. (c) Shimizu, K.; Cha, J.; Stucky, G. D.; Morse, D. E. *Proc. Natl. Acad. Sci. U.S.A.* **1998**, *95*, 6234−6238. (d) Tacke, R. *Angew. Chem., Int. Ed.* **1999**, *38*, 3015−3018.
(4) (a) Noll, W. *Chemistry and Technology of the Silicones*; Academic Press: New York, 1968. (b) Clarson, S. J., Semlyen, J. A., Eds. *Siloxane Polymers*; Prentice Hall: Englewood Cliffs, NJ, 1993.
(5) (a) Okumoto, S.; Fujita, N.; Yamabe, S. *J. Phys. Chem. A* **1998**, *102*, 3991−3998. (b) Kudo, T.; Gordon, M. S. *J. Am. Chem. Soc.* **1998**, *120*, 11432−11438. (c) Kudo, T.; Gordon, M. S. *J. Phys. Chem. A* **2000**, *104*, 4058−4063. (d) Kudo, T.; Gordon, M. S. *J. Phys. Chem. A* **2002**, *106*, 11347−11353.
(6) (a) Lickiss, P. D. *Adv. Inorg. Chem.* **1995**, *42*, 147−262. (b) Chandrasekhar, V.; Boomishankar, R.; Nagendran, S. *Chem. Rev.* **2004**, *104*, 5847−5910.
(7) (a) Bourne, S. A.; Nassimbeni, L. R.; Skobridis, K.; Weber, E. *J. Chem. Soc., Chem. Commun.* **1991**, 282−283. (b) Schneider, M.; Neumann, B.; Stammler, H. G.; Jutzi, P. *Monatsh. Chem.* **1999**, *130*, 33−44.
(8) (a) Babaian, E. A.; Huff, M.; Tibbals, F. A.; Hrncir, D. C. *J. Chem. Soc., Chem. Commun.* **1990**, 306−307. (b) Bourne, S. A.; Johnson, L.; Marais, C.; Nassimbeni, L. R.; Weber, E.; Skobridis, K.; Toda, F. *J. Chem. Soc., Perkin Trans. 2* **1991**, 1707−1713. (c) Bowes, K. F.; Glidewell, C.; Low, J. N. *Acta Crystallogr.* **2002**, *C58*, o409−o415.
(9) (a) Ruud, K. A.; Sepeda, J. S.; Tibbals, F. A.; Hrncir, D. C. *J. Chem. Soc., Chem. Commun.* **1991**, 629−630. (b) Baxter, I.; Cother, L. D.; Dupuy, C.; Lickiss, P. D.; White, A. J. P.; Williams, D. J. http://www.ch.ic.ac.uk/ectoc/ectoc-3/pub/010/index.html, 1997; accessed on Dec. 4, 2002. (c) O'Leary, B.; Spalding, T. R.; Ferguson, G.; Glidewell, C. *Acta Crystallogr.* **2000**, *B56*, 273−286. (d) Goeta, A. E.; Lawrence, S. E.; Meehan, M. M.; O'Dowd, A.; Spalding, T. R. *Polyhedron* **2002**, *21*, 1689−1694. (e) Klingebiel, U.; Neugebauer, P.; Müller, I.; Noltemeyer, M.; Usón, I. *Eur. J. Inorg. Chem.* **2002**, 717−722. (f) Bowes, K. F.; Ferguson, G.; Lough, A. J.; Glidewell, C. *Acta Crystallogr.* **2003**, *B59*, 277−286. (g) Turkington, D. E.; Lough, A. J.; Ferguson, G.; Glidewell, C. *Acta Crystallogr.* **2004**, *B60*, 238−248. (h) Prabusankar, G.; Murugavel, R.; Butcher, R. J. *Organometallics* **2004**, *23*, 2305−2314.
(10) (a) Ugliengo, P.; Bleiber, A.; Garrone, E.; Sauer, J.; Ferrari, A. M. *Chem. Phys. Lett.* **1992**, *191*, 537−547. (b) Cypryk, M. *J. Organomet. Chem.* **1997**, *545−546*, 483−493. (c) Cypryk, M.; Apeloig, Y. *Organometallics* **2002**, *21*, 2165−2175. (b) Ignatyev, I. S.; Partal, F.; López González, J. J. *J. Phys. Chem. A* **2002**, *106*, 11644−11652. (d) Thompson, K. C.; Margey, P. *Phys. Chem. Chem. Phys.* **2003**, *5*, 2970−2975. (e) Ignatyev, I. S.; Partal, F.; López González, J. J. *Chem. Phys. Lett.* **2004**, *384*, 326. (f) Ignatyev, I. S. *Spectrochim. Acta A* **2004**, *60*, 1169−1178. (g) Ignatyev, I. S.; Montejo, M.; Partal Ureña, F.; López González, J. J. *Chem. Phys. Lett.* **2005**, *412*, 359−364. (h) Cypryk, M. *J. Phys. Chem. A* **2005**, *109*, 12020−12026. (i) Delak, K. M.; Sahai, N. *J. Phys. Chem. B* **2006**, *110*, 17819−17829.
(11) (a) Beckmann, J.; Duthie, A.; Reeske, G.; Schürmann, M. *Organometallics* **2004**, *23*, 4630−4635. (b) Beckmann, J.; Jänicke, S. L. *Eur. J. Inorg. Chem.* **2006**, 3351−3358. (c) Beckmann, J.; Jänicke, S. L. Submitted for publication.
(12) *Gaussian W03*, Revision B.04; Gaussian: Pittsburgh, PA, 2003.
(13) Anderson, M. P.; Uvdal, P. *J. Phys. Chem. A* **2005**, *109*, 2937−2941.

Supramolecular Silanol Chemistry in the Gas Phase

J. Phys. Chem. A, Vol. 111, No. 10, 2007 **2019**

(14) Boys, S. F.; Bernardi, F. *Mol. Phys.* **1970**, *19*, 553−566.

(15) Bader, R. F. W. *Atoms in Molecules—A Quantum Theory*; Oxford University Press: Oxford, U.K., 1990.

(16) Biegler-König, F.; Schönbohm, J. *J. Comput. Chem.* **2002**, *23*, 1489−1494.

(17) Reed, A. E.; Curtiss, A. E.; Weinhold, F. *Chem. Rev.* **1988**, *88*, 899−926.

(18) Glendening, E. D.; Reed, A. E.; Carpenter, J. E.; Weinhold, F. *NBO*, Version 3.1.

(19) (a) West, R.; Whatley, L. S.; Lake, K. J. *J. Am. Chem. Soc.* **1961**, *83*, 761−764. (b) Pitt, C. G.; Bursey, M. M.; Chatfield, D. A. *J. Chem. Soc., Perkin Trans. 2* **1976**, 434−438. (c) Shambayati, S.; Blake, J. F.; Wierschke, S. G.; Jorgensen, W. L.; Schreiber, S. L. *J. Am. Chem. Soc.* **1990**, *112*, 697−703. (d) Blake, J. F.; Jorgensen, W. L. *J. Org. Chem.* **1991**, *56*, 6052−6059.

(20) (a) Tielens, F.; De Proft, F.; Geerlings, P. *J. Mol. Struct. (THEOCHEM)* **2001**, *542*, 227−237. (b) Beckmann, J.; Dakternieks, D.; Lim, A. E. K.; Lim, K. F.; Jurkschat, K. *J. Mol. Struct.* (*THEOCHEM*) **2006**, *761*, 177−193.

(21) Beckmann, J.; Grabowsky, S.; Thöne, M. Manuscript in preparation.

(22) Steiner, T. *Angew. Chem., Int. Ed.* **2002**, *41*, 48−76.

(23) Ludwig, R. *Angew. Chem., Int. Ed.* **2001**, *40*, 1808−1827.

(24) Puff, H.; Braun, K.; Reuter, H. *J. Organomet. Chem.* **1991**, *409*, 119−219.

(25) (a) West, R.; Baney, R. H. *J. Am. Chem. Soc.* **1959**, *81*, 6145−6148. (b) Dijkstra, T. W.; Duchateau, R.; van Santen, R. A.; Meetsma, A.; Yap, G. P. A. *J. Am. Chem. Soc.* **2002**, *124*, 9856−9864.

(26) (a) Koch, U.; Popelier, P. L. A. *J. Phys. Chem.* **1995**, *99*, 9747−9754. (b) Popelier, P. L. A. *J. Phys. Chem. A* **1998**, *102*, 1873−1878. (c) Grabowski, S. *Chem. Phys. Lett.* **2001**, *338*, 361−366. (d) Kolandaivel, P.; Nirmala, V. *J. Mol. Chem.* **2004**, *694*, 33−38. (e) Parthasarathi, R.; Subramanian, V.; Sathyamurthy, N. *J. Phys. Chem A* **2006**, *110*, 3349−3351. (f) Ziolkowski, M.; Grabowski, S.; Leszcynski, J. *J. Phys. Chem. A* **2006**, *110*, 6514−6521.

(27) Weinhold, F. *J. Mol. Struct. (THEOCHEM)* **1997**, *398−399*, 181−197.

(28) Gillespie, R. J.; Johnson, S. A. *Inorg. Chem.* **1997**, *36*, 3031−3039.

(29) Jakubikova, E.; Rappé, A. K.; Bernstein, E. R. *J. Phys. Chem. A* **2006**, *110*, 9529−9541.